

Microfluidic Directed Self-Assembly of Liposome-Hydrogel Hybrid Nanoparticles

Jennifer S. Hong^{1,3}, Samuel M. Stavis¹, Silvia H. DePaoli Lacerda⁵, Laurie E. Locascio², Srinivasa R. Raghavan⁴, and Michael Gaitan¹

¹Semiconductor Electronics Division and ²Biochemical Science Division, National Institute of Standards and Technology, Gaithersburg, MD;

³Department of Bioengineering and ⁴Department of Chemical and Biomolecular Engineering, University of Maryland, College Park, MD;

⁵Center for Biologics Evaluation and Research, Food and Drug Administration, Bethesda, MD

jennifer.hong@nist.gov

Abstract

We present a microfluidic method to direct the self-assembly of temperature-sensitive liposome-hydrogel hybrid nanoparticles. Our approach yields nanoparticles with structural properties and highly monodisperse size distributions precisely controlled across a broad range relevant to the targeted delivery and controlled release of encapsulated therapeutic agents. We used microfluidic hydrodynamic focusing to control the convective-diffusive mixing of two miscible nanoparticle precursor solutions (a DPPC:Cholesterol:DCP phospholipid formulation in isopropanol, and a photopolymerizable N-Isopropylacrylamide mixture in aqueous buffer) to form nanoscale lipid vesicles with encapsulated hydrogel precursors. These precursor nanoparticles were collected off-chip and were UV-irradiated in bulk to polymerize the nanoparticle interiors into hydrogel cores. Multi-angle laser light scattering in conjunction with asymmetric flow field-flow fractionation was used to characterize nanoparticle size distributions, which spanned the ≈ 150 to ≈ 300 nm diameter range as controlled by microfluidic mixing conditions, with a polydispersity of ≈ 3 % to ≈ 5 % (relative standard deviation). Transmission electron microscopy was then used to confirm the spherical shape and core-shell composition of the hybrid nanoparticles. This method may be extended to the

directed self-assembly of other hybrid nanoparticle systems with engineered size/structure-function relationships to advance the success of soft matter nanoparticles for practical use in healthcare and life science applications.

Introduction

Soft matter nanoparticles such as nanoscale lipid vesicles, hydrogel nanoparticles, and hybrids of the two have many important applications in healthcare and the life sciences^{1,2}. Such nanoparticles have been applied in areas of single molecule manipulation and metrology³, sensors⁴, biomedical imaging⁵, and chromatography⁶. Particular interest has grown in developing methods for the synthesis of soft nanoparticles as potential carriers for the targeted delivery and controlled release of therapeutic agents for diagnostic and treatment purposes⁷⁻¹¹. Although many types of these nanoparticles have been developed, few have advanced to clinical use because of a lack of consistent toxicology data, which in turn arises partly because nanoparticle preparation techniques yield erratic results across laboratories¹².

Soft nanoparticles are predominantly synthesized using bulk techniques. Phospholipid-based nanoparticles are typically prepared using evaporation-rehydration or solvent-injection methods, while polymeric nanoparticles are traditionally synthesized using emulsification or solvent-evaporation methods¹³⁻¹⁵. The technical limitations associated with bulk methods for synthesizing soft nanoparticles constitute a significant impediment to the realization of many of the aforementioned applications. These limitations include nanoparticle size distributions that are polydisperse, irreproducible from batch to batch, and strongly dependent on chemical formulation^{11,16}. A root cause of these problems is the disparity between macroscopic control over the reaction of nanoparticle precursor solutions and the microscopic fluid environment which determines the formation of nanoparticles. These limitations often necessitate the use of post-processing techniques such as high-frequency sonication, freeze-thaw cycling, or membrane-extrusion to homogenize nanoparticle size and composition, which can decrease yield, increase assembly time, and be incompatible with biological applications⁶.

To address these limitations, a variety of microfluidic methods have recently been developed to synthesize soft matter nanoparticles with improved control over size distribution, as size has been determined to be a critical factor in influencing nanoparticle efficacy or toxicity for a particular application^{12,17,18}. One such method is the use of microfluidic hydrodynamic focusing¹⁹ to precisely control the convective-diffusive mixing of miscible liquids at nanometer length scales and microsecond time scales which determine the formation of nanoparticles. This technique has been used to direct the self-assembly of lipid molecules into nanoscale lipid vesicles of controlled size in a continuous and reproducible manner²⁰, obviating the need for post-processing to homogenize nanoparticle size. Similar microfluidic approaches have been used to produce polymeric nanoparticles^{11,21}.

Beyond these single-material lipid or polymer nanoparticle systems that have been synthesized using microfluidic devices, relatively few microfluidic methods for the precisely controlled synthesis of multiple-material hybrid nanoparticle systems have been demonstrated, despite the important applications thereof. In particular, liposome-hydrogel hybrid nanoparticles, also known as lipobeads, combine many of the advantageous material properties of the individual constituents for therapeutic applications^{2,6,22-25}. The hydrogel interior improves both the mechanical stability of hybrid liposome-hydrogel nanoparticles and the controlled release of encapsulated therapeutic agents, while the many useful surface properties of the exterior lipid vesicle are retained for both stealth capability and targeted delivery^{14,26-30}. This potential therapeutic utility motivates the development of advanced microfluidic methods to control the synthesis of these more structurally complex soft matter nanostructures.

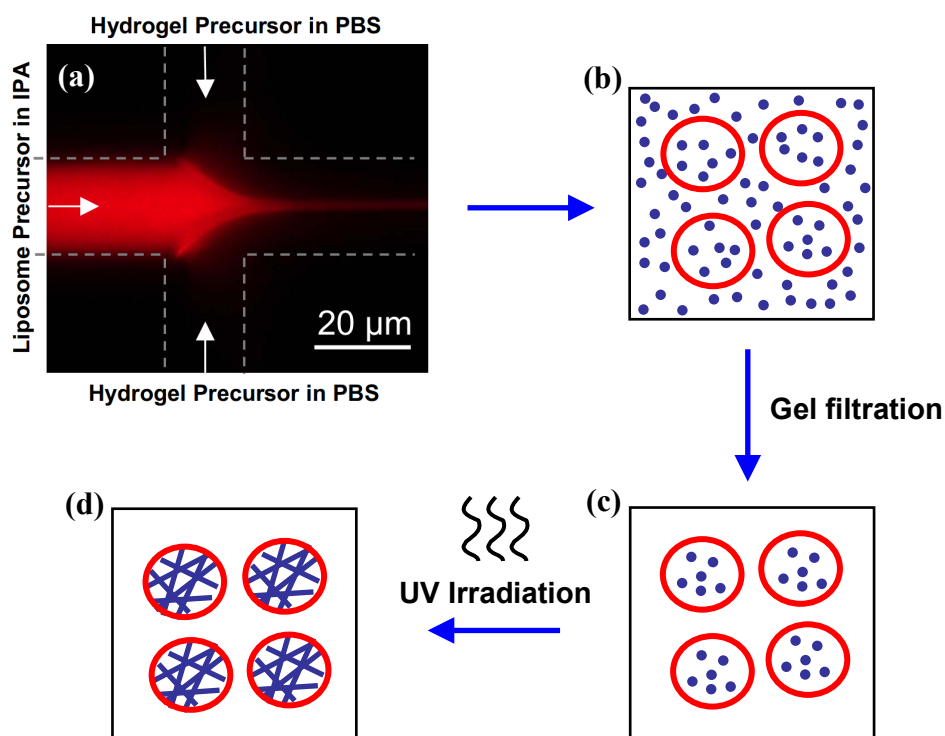


Figure 1. Schematic depicting the on-chip microfluidic directed self assembly and off-chip polymerization of liposome-PNIPA hydrogel nanoparticles. (a) A solution of lipid and lipophilic tracer DiD (red) dissolved in IPA was hydrodynamically focused by a solution of the hydrogel precursor in buffer. Microfluidic mixing was used to direct the formation of nanoscale lipid vesicles with encapsulated gel precursors, and the sample was collected (b) at the device outlet. (c) The extravascular gel precursor material was removed by gel filtration, and the particles were resuspended in buffer. (d) Subsequent UV irradiation initiated the free-radical polymerization of the liposome interior which produced liposome-PNIPA hydrogel nanoparticles.

In this manuscript, we present a microfluidic approach to the directed self-assembly of monodisperse liposome-hydrogel hybrid nanoparticles of controlled size.

We selected poly(N-isopropylacrylamide) (PNIPA) as our model polymer, as it is one of the most widely studied thermo-responsive polymers for therapeutic applications and also because it has been used recently for the bulk formation of lipobeads³¹⁻³⁴. As shown in Figure 1, our approach utilizes microfluidic hydrodynamic focusing to control the diffusive mixing of two miscible liquids³⁵ that separately contain the precursors to our hybrid nanoparticles. One solution contains a mixture of phospholipids and cholesterol in isopropanol (IPA) and forms the central stream in Figure 1a. The outer sheath flow consists of an aqueous solution of N-isopropylacrylamide (NIPA), crosslinker, and free-radical initiator, in phosphate-buffered saline (PBS).

Using this approach, we can direct the assembly of liposomes at the interface between the two streams, and these liposomes encapsulate the contents of the aqueous solution; *i.e.*, the hydrogel precursors. Moreover, by varying the volumetric flow-rate-ratio (VFRR) of the aqueous outer streams to the central lipid-IPA stream, the convective-diffusive mixing conditions at the interface are altered, and thereby the size of the liposomes can be controlled. The liposomes at the outlet of the microfluidic chip are then collected, purified by gel filtration, and UV-irradiated off-chip to polymerize the encapsulated precursors into a hydrogel core. Hybrid nanoparticles of controlled size can thus be prepared in the 150 nm to 300 nm diameter range with a polydispersity of <5 % (relative standard deviation). This approach can be extended to the assembly of other hybrid nanoparticle systems of interest³⁶. Microfluidic assembly may offer greater control over nanoparticle size and compositional requirements, **as well as provide a platform that potentially enables the systematic characterization of different nanoparticle formulations.**

Experimental Section³⁷

Materials. The lipid dye 1,1'-dioctadecyl-3,3,3',3'-tetramethylindodicarbocyanine perchlorate (DiD) was obtained from Molecular Probes (Eugene, OR), and 1,2-dipalmitoyl-*sn*-glycero-3-phosphocholine (DPPC) and cholesterol from Avanti Polar Lipids (Alabaster, AL). Dihexadecyl phosphate (DCP), N-isopropylacrylamide (NIPA)

(97 % purity), N,N'-methylenebis(acrylamide) (MBA) (99 % purity), 2,2-diethoxyacetophenone (DEAP) (purity >95% GC), and sodium azide (NaN_3) were obtained from Sigma-Aldrich. Polydimethylsiloxane (PDMS) (Sylgard 184) was purchased from Dow Corning. Hamilton gas-tight glass syringes and anotop syringe filters were obtained from Fisher Scientific. D-Salt columns were purchased from Pierce (Rockford, IL).

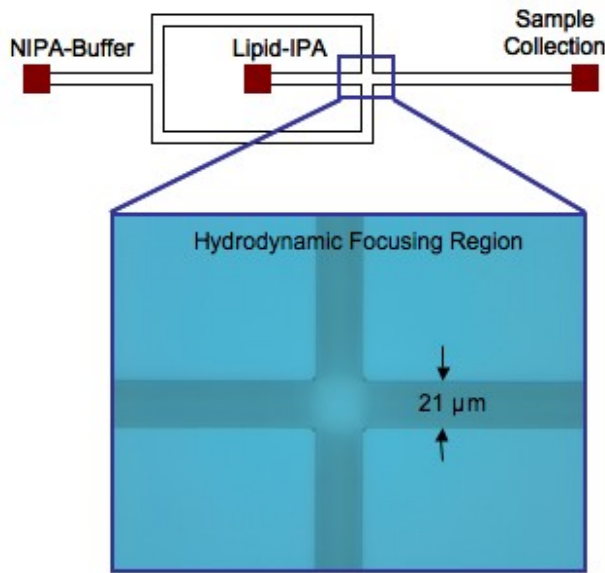


Figure 2. Device schematic and optical micrograph of the microfluidic hydrodynamic focusing cross junction. Microchannels were fabricated in a silicon substrate which was anodically bonded to a borosilicate glass cover. The microfluidic channel was $(21 \pm 1) \mu\text{m}$ wide and $(39 \pm 1) \mu\text{m}$ deep (mean \pm expanded uncertainty).

Microfluidic Device Fabrication. A schematic and brightfield micrograph of the microfluidic device is shown in Figure 2. Microfluidic devices were constructed using standard photolithographic microfabrication processes. A thin film of positive tone photoresist was spin-coated onto the front side of a double-side-polished silicon substrate wafer with a thickness of $\approx 290 \mu\text{m}$. Networks of fluidic channels with widths of $(21 \pm 1) \mu\text{m}$ (mean \pm expanded uncertainty) were patterned in the photoresist using contact photolithography. Device patterns were transferred into the substrate using Bosch Process deep reactive ion etching to a depth of $(39 \pm 1) \mu\text{m}$ (mean \pm expanded

uncertainty). A thin film of silicon dioxide was deposited as an etch stop on the front side of the substrate using plasma-enhanced chemical vapor deposition. A thin film of positive tone photoresist was spin-coated onto the back side of the substrate, and a second layer of contact photolithography was used to pattern access holes aligned to the channel inlets and outlets. Access holes were then formed by deep reactive ion etching of the substrate through to the etch stop. The substrate wafer was immersed in buffered hydrofluoric acid to remove the silicon dioxide etch stop and finally cleaned with a mixture of ammonium hydroxide:hydrogen peroxide:water ($\approx 5:1:1$ volume ratio) at a temperature of ≈ 80 °C. A borosilicate glass cover wafer with a thickness of ≈ 170 μm was anodically bonded to the front side of the substrate wafer to form enclosed microfluidic channels. Fluidic connectors were adhered to the backside of the substrate wafer to couple polyetheretherketone capillaries to the inlets and outlets of the microfluidic devices. The opposing end of each inlet capillary was attached to a gastight glass Hamilton syringe filled with reagent. The syringes were mounted onto syringe pumps (Harvard Apparatus, MA) to control continuous fluid flow into the microchannels.

Epifluorescence Microscopy. An inverted optical microscope was used in epifluorescence mode to observe microfluidic formation of nanostructures. Microfluidic flow was imaged through the cover wafer with a plan apochromat air immersion objective of magnification $40\times$ and numerical aperture 0.95. A metal halide arc lamp was used with a 625 nm to 655 nm band pass filter for fluorescence excitation, and fluorescence emission was isolated with a 660 nm dichroic mirror and refined with a 665 nm to 715 nm band pass filter. Videos and images were acquired with either an electron multiplying or color charge coupled device camera. Following nanoparticle synthesis experiments, hybrid nanoparticles were suspended on a glass coverslip with a thickness of ≈ 170 μm for inspection using the same optical setup.

Buffer Preparation. 0.01 mmol/L Phosphate buffered saline (PBS) (0.138 mol/L NaCl, 2.7 mmol/L KCl, pH 7.4) was used in all experiments unless otherwise specified. PBS was prepared in 18.2 M Ω filtered deionized water with the addition of 3 mmol/L NaN_3 to

prevent bacterial growth. All PBS solutions were filtered through a 0.1 μm syringe filter prior to use in sample preparation.

Lipid and Hydrogel Precursor Preparation. A mixture of DPPC:cholesterol:DCP (7:2:1 molar ratio) and 0.5 mol% DiD lipophilic tracer was used in the formation of the empty liposomes and liposome-hydrogel hybrid nanoparticles. The mixture was dissolved in chloroform in a glass scintillation vial and was dried down under dry nitrogen for 45 min to produce a thin lipid film, and the dried lipid film was placed in a vacuum desiccator overnight to remove any residual solvent. The NIPA:MBA:DEAP (3.5%:0.35%:0.1% weight per volume ratio) gel precursor solution was prepared in PBS. An Omnicure S2000 (EXFO Life Sciences, Canada) lamp ($\lambda = 365 \text{ nm}$; 40 W cm^{-2}) was used to initiate free-radical polymerization of the bulk hydrogel precursor material. The onset of polymerization was observed immediately upon UV irradiation, and complete bulk gel formation was verified after 15 min of irradiation.

Precursors to Hybrid Nanoparticles by Microfluidic Flow Focusing.

Nanoscale liposomes containing hydrogel precursors were synthesized using microfluidic mixing controlled by hydrodynamic focusing³⁵. The lipid film was redissolved in dry 0.1 μm filtered IPA to obtain a 6.25 mmol/L solution. The lipid solution and either the gel precursor (experimental) or PBS (control) solution were each loaded in a glass syringe and connected to the device inlets, as shown in Figure 2. Syringe pumps were used to control the flow of lipid-IPA solution into the center channel and PBS or gel precursor solution into the side channels to hydrodynamically focus the lipid-IPA stream, shown in Figure 1a. Empty liposomes were formed in PBS at VFRRs of 10:1, 15:1, 20:1, and 25:1, while liposomes encapsulating the gel precursor were formed at VFRRs of 10:1, 15:1, and 25:1. The total volumetric flow rate was held constant at 9.6 $\mu\text{L}/\text{min}$ in all cases. Samples were collected at the device outlet for 55 min following 10 min of stabilization at each VFRR setting.

Off-Chip Formation of Hybrid Nanoparticles.

Liposomes encapsulating the gel precursor were passed through a D-Salt polyacrylamide column (6 kDa cutoff), using PBS as the elution buffer, to remove the extravesicular gel precursor material from the sample. PDMS wells (1.6 cm diameter x 0.3 cm height) were stamped and cut from a cured PDMS sheet, and the wells were cleaned with ethanol followed by deionized water. They were dried with nitrogen before being placed on a glass microscope slide. Added to each well were 0.5 mL aliquots of sample, which were also irradiated with UV light at 365 nm from the Omnicure S2000 for 15 min.

Asymmetric Flow Field-Flow Fractionation and Multi-Angle Laser Light Scattering (AF4-MALLS).

An Eclipse AF4-MALLS instrument was used for size fractionation and characterization of the liposomes and nanoparticles. The AF4 separation channel had a 190 μm spacer, and a regenerated cellulose membrane with a 10 kDa cutoff was used for the cross-flow partition. For the control liposomes, 10 mmol/L PBS was used as the carrier solution. Ten μL of the liposome solution was loaded into the AF4 injection loop, and the fractionation was conducted with a 1 mL/min channel flow and a 0.8 mL/min to 0.0 mL/min linearly decreasing crossflow gradient over 70 min. For the hybrid nanoparticles, a 5 mmol/L PBS carrier solution, a 50 μL sample injection, and a 0.6 mL/min to 0.0 mL/min linearly decreasing crossflow gradient over a 35 min elution period were used. MALLS data were collected simultaneously at 10 scattering angles on the eluting sample. A coated sphere model³⁸ was applied to the data using an estimated bilayer thickness of 5 nm to determine the geometric radii distributions of liposomes and hybrid nanoparticles.

Dynamic Light Scattering (DLS).

A 90Plus/BI-MAS Particle Size Analyzer instrument was used for DLS measurements (Brookhaven Instruments). The instrument was equipped with a 15 mW solid state laser with a wavelength of 659 nm, and measurements were made at 90° at a rate of one measurement per second. Nanoparticle samples were centrifuged at 10000 rpm for 4 min to remove any dust or aggregates prior to measurement. The supernatant was then aspirated and diluted 1:10 in 0.02 μm filtered PBS, and the sample was added to

a polymethylmethacrylate cuvette and placed in the measurement cell. Measurements were made over a series of temperatures.

Transmission Electron Microscopy (TEM).

TEM of the hybrid nanoparticles was performed on a Philips EM 400T microscope operating at 120 kV equipped with a Soft Imaging System CCD camera (Cantega 2K). TEM samples were prepared by dropping diluted solutions onto 400-mesh carbon-coated copper grids (from Ted Pella) and briefly air-drying the samples prior to measurements.

Results and Discussion

Empty Liposomes in PBS.

Empty liposomes, prepared in PBS without the hydrogel precursor, were synthesized in the microfluidic device as a calibration to determine the size ranges achieved at varying volumetric flow-rate ratios (VFRRs) with our device geometry and lipid formulation. Under the laminar flow conditions typical at microfluidic length-scales, the mixing of miscible liquids flowing in parallel streams occurs predominantly by molecular diffusion, as influenced by convection in our system. In both the hydrodynamic focusing region and in the downstream mixing channel, IPA diffused into the buffer and vice-versa to the point where the concentration of lipid exceeded its critical micelle concentration and caused the lipids to self-assemble into vesicle bilayers, thus shielding the hydrophobic moieties from water. As the liposomes self-assembled, the vesicles encapsulated the surrounding buffer or hydrogel precursor mixture into the aqueous vesicle core.

The critical mixing time over which this self-assembly process occurred was dependent on the extent of focusing of the center stream.³⁵ At lower focusing, or smaller VFRRs, the center lipid-IPA stream was relatively wide with a low surface-to-volume ratio between the lipid stream and sheath flows, requiring a longer diffusive mixing time

to deplete the center stream. The prolonged lipid solubility resulted in the self-assembly of larger vesicles further downstream in the diffusive mixing channel while fewer vesicles formed in the focusing region. At higher focusing, or larger VFRRs, convective flow resulted in a relatively narrow center stream, which reduced the diffusion distance and enhanced diffusive mixing in the hydrodynamic focusing region. Higher focusing also resulted in a higher surface-to-volume ratio and a faster depletion of the center stream. This caused the self-assembly of smaller liposomes predominantly within the hydrodynamic focusing region as opposed to downstream in the mixing channel. Control of these flow conditions enabled predictable and repeatable steady-state mixing and the continuous production of liposome and precursor hybrid nanoparticle size distributions.

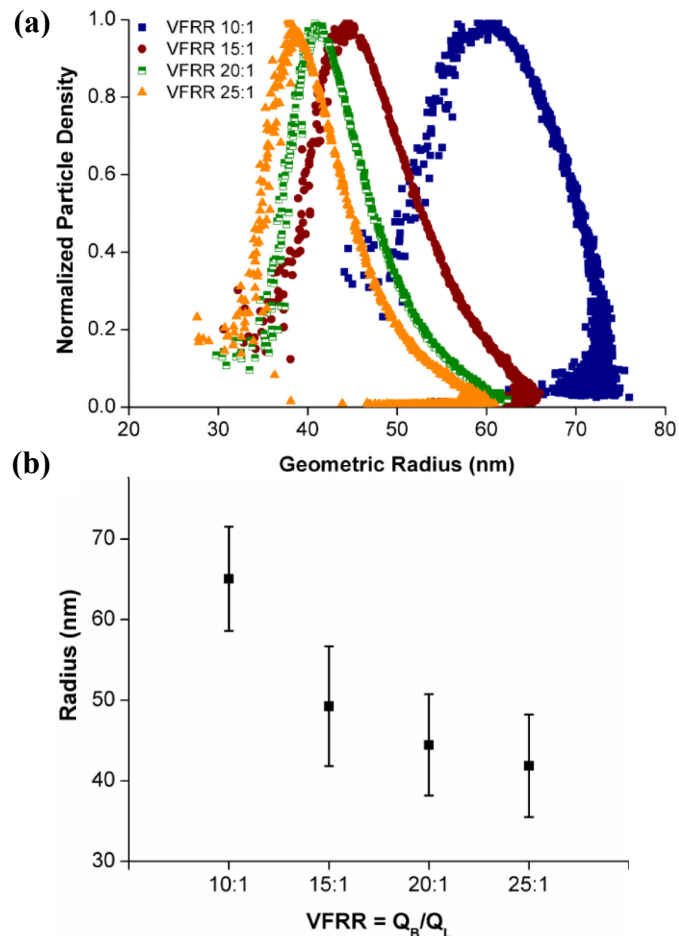


Figure 3. (a) Size distributions measured by AF4-MALLS of empty liposome populations formed in PBS alone by hydrodynamic focusing at varying VFRRs. (b) The average outer vesicle radius and standard deviation of each population are shown. Q_B and Q_L denote the volumetric flow rates of the buffer and lipid-IPA, respectively.

The liposomes were formed at VFRRs of 10:1, 15:1, 20:1, and 25:1, and the collected samples were characterized by AF4-MALLS. The size distribution of each VFRR sample is shown in Figure 3a. Here, for a given sample, each data point represents a MALLS measurement of a size-fractionated component; thereby, the overall size distribution is a more accurate characterization of the sample compared to that obtained from traditional static or dynamic light scattering³⁹. The size distributions show the expected trend where an increase in VFRR results in a smaller size distribution of liposomes⁴⁰. For a simplified view of this trend, Figure 3b plots the average radius and polydispersity vs. VFRR. In calculating these averages, the sizes were weighted by the number density data from Figure 3a. The average radius and standard deviation of the distributions for the 10:1, 15:1, 20:1, and 25:1 samples were (65±6) nm, (49±7) nm, (44±6) nm, and (41±6) nm, respectively. These numbers indicate that each liposome population is narrowly dispersed, particularly when compared to other liposome preparation techniques³⁵. At VFRRs 20:1 and 25:1, the size varies only slightly, suggesting that we are approaching the lower limit of liposome size that can be produced for this formulation in our microfluidic device. These results guided our selection of VFRR settings for the formation of the liposome-PNIPA hybrid nanoparticles.

Liposome-PNIPA Hybrid Nanoparticles.

Due to the incremental difference in average vesicle size from the empty liposome synthesis experiments between VFRRs 15:1 and 20:1, and more so between 20:1 and 25:1, the 20:1 VFRR was omitted from the hybrid nanoparticle formation run. Liposomes encapsulating the NIPA:MBA:DEAP hydrogel precursor solution were formed in a single continuous-flow run at VFRRs of 10:1, 15:1, and 25:1.

Compared to the formation of the liposomes in PBS alone, transient chemical interactions arising from phase separation of the precursor components occurred more

frequently at the hydrodynamic interface between the lipid and hydrogel precursor streams, especially closer to the borosilicate glass surface of the device. Such interfacial buildup occurred at all three VFRR formation settings but did not disrupt the directed assembly of precursor hybrid nanoparticles. This issue was more problematic in trials with significantly higher hydrogel precursor concentration (data not shown), however, providing some insight into the limitations of our technique.

The liposomes collected at the outlet of the microfluidic chip were purified by gel filtration and then UV polymerized to yield liposome-PNIPA hybrid nanoparticles (Figure 1). The size distributions of these nanoparticle samples were then measured by AF4-MALLS and are shown in Figure 4. The liposomes containing NIPA before UV irradiation were also characterized, and those results (Figure 4a) indicate structures with low polydispersities comparable to the empty liposomes. Polymerization does not alter the average size appreciably, and the final liposome-PNIPA hybrid nanogels actually have even narrower size distributions, as shown in Figure 4b. This holds true at each of the applied VFRRs, spanning an overall size range of about 150 nm to 300 nm in diameter. The average radius and polydispersity for each VFRR is shown in Figure 4c; these were (142 ± 4) nm, (109 ± 3) nm, and (92 ± 5) nm for VFRRs of 10:1, 15:1, and 25:1, respectively.

An interesting point is that, at a given VFRR, liposomes containing the NIPA precursor mixture were approximately twice the size of empty liposomes (compare Figures 3a and 4a). The similarity in size distributions in Figures 4a and 4b indicates that this discrepancy from the empty liposomes size distributions was not caused by UV polymerization, but was rather a result of changes in the microfluidic chemical environment caused by the addition of the hydrogel precursor molecules in the aqueous stream, which evidently altered the conditions of the molecular self-assembly and encapsulation processes.

The formation of liposome-PNIPA nanoparticles by our approach showed a batch-to-batch reproducibility in size to within 5 % to 15 % as measured by AF4-MALLS. This variability was attributed to experimental variation in convective flow conditions as well as the transient chemical interactions observed between the hydrogel

and liposome precursor streams during the continuous formation of precursor hybrid nanoparticle samples.

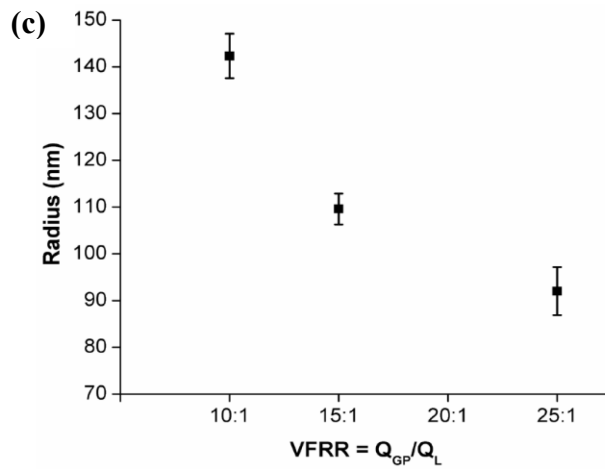
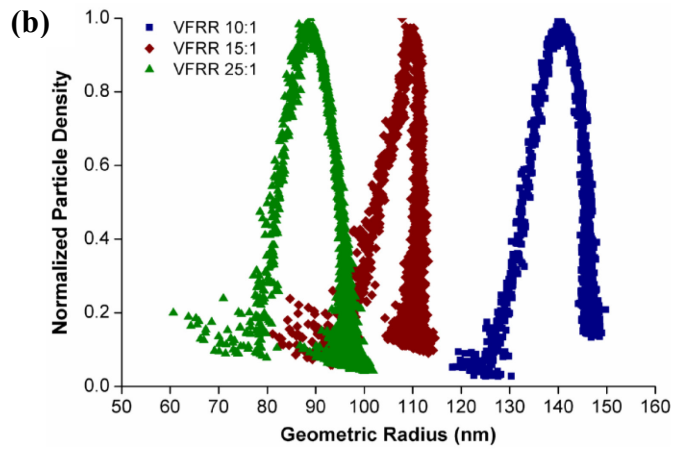
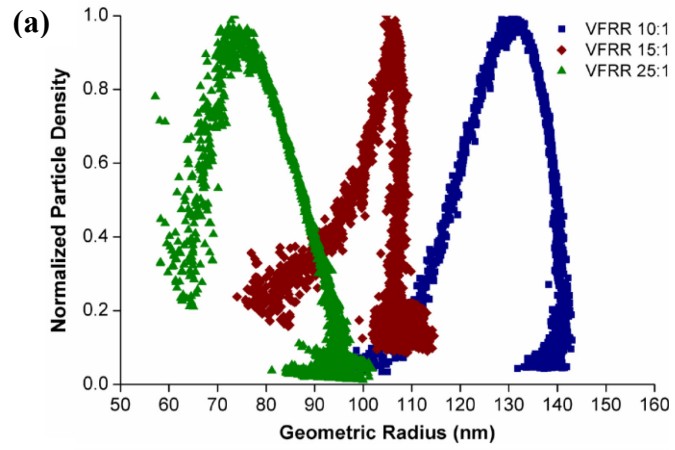


Figure 4. (a) Size distributions of lipid-NIPA liposomes; and (b) liposome-PNIPA hybrid nanoparticles formed by polymerizing the liposomes in (a). (c) Average liposome-PNIPA hybrid nanoparticle size at varying VFRRs. Q_{GP} and Q_L denote the flow rates of the gel precursor and lipid solutions, respectively. The small standard deviation for each population illustrates the narrow size distributions achieved by our microfluidic directed self-assembly method.

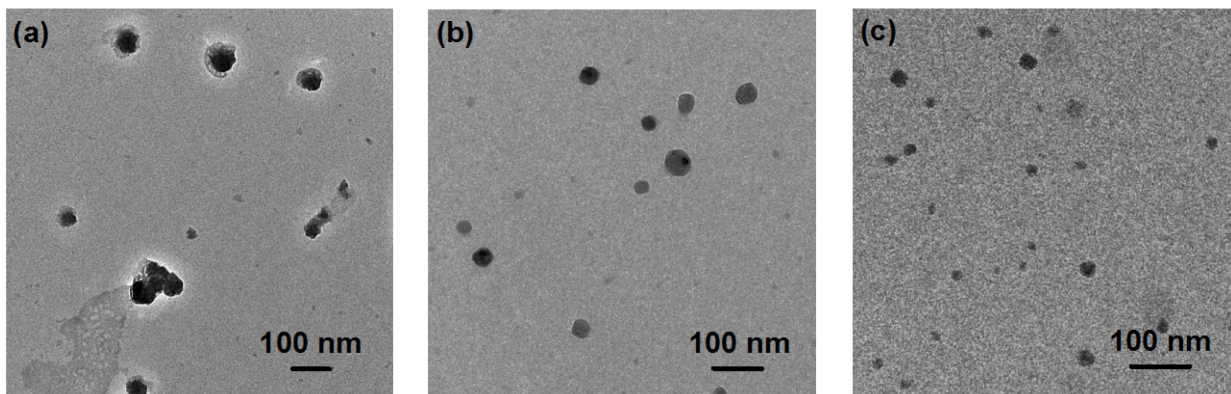


Figure 5. TEM micrographs of liposome-PNIPA hybrid nanoparticles formed at varying VFRRs of (a) 10:1, (b) 15:1, and (c) 25:1. The nanoparticles exhibit characteristics of solid spherical structures and show a trend of decreasing size with increasing VFRR.

The hybrid nanoparticles were also characterized by TEM (Figure 5). Each sample was air-dried on a TEM grid prior to imaging, and the micrographs in Figure 5 therefore correspond to dehydrated nanoparticles. The hybrid nanoparticles were uniformly solid and exhibited the round shape of the liposome envelope, which confirms the successful encapsulation and polymerization of the hydrogel precursor within the liposomal interior. The particle size exhibits a decrease with an increase in VFRR, as earlier demonstrated by AF4-MALLS. These sizes are much smaller than those shown in Figure 4, which is attributed to the dehydration of the liposome-PNIPA nanoparticles.

Temperature Sensitivity of Liposome-PNIPA Nanoparticles.

To further validate the solid core composition of the liposome-PNIPA nanoparticles produced by our microfluidic synthesis strategy, we investigated the temperature-sensitivity of particles synthesized at a VFRR of 10:1 using DLS. It is

known that PNIPA exhibits a lower critical solution temperature (LCST) in water, and, as a result, PNIPA hydrogels shrink when heated up to its LCST, which is $\approx 32\text{ }^{\circ}\text{C}$ ^{41,42}. Therefore, we measured the size of liposome-PNIPA hydrogel nanoparticles over a range from $25\text{ }^{\circ}\text{C}$ to $32\text{ }^{\circ}\text{C}$, and then at $37\text{ }^{\circ}\text{C}$, which is the physiological temperature at which these nanoparticles may potentially be applied. At each temperature, the sample was equilibrated, and three measurement runs were performed. The average values of the hydrodynamic diameter D_h from DLS along with the standard deviations are plotted in Figure 6. The average D_h was (260 ± 10) nm at $25\text{ }^{\circ}\text{C}$, (243 ± 7) nm at $32\text{ }^{\circ}\text{C}$, and at $37\text{ }^{\circ}\text{C}$ was (224 ± 7) nm. These results show the characteristic temperature response of PNIPA, with the size decreasing past the LCST ($32\text{ }^{\circ}\text{C}$). Similar results have been reported for liposome-PNIPA hybrid particles prepared by a bulk method³⁴.

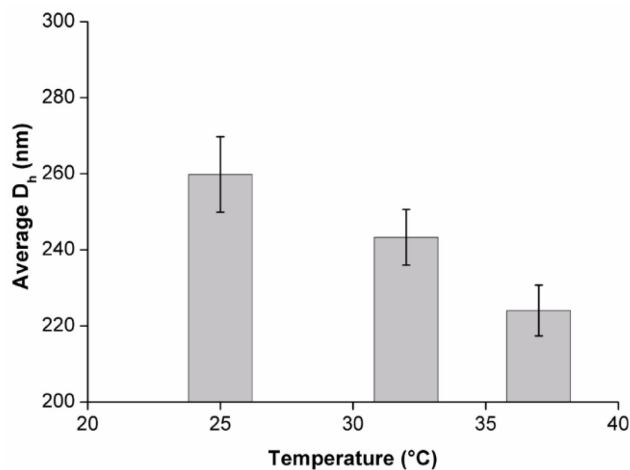


Figure 6. DLS data showing the effect of increasing temperature on the hydrodynamic diameter D_h of liposome-PNIPA hybrid nanoparticles prepared at a VFRR of 10:1.

Another interesting phenomenon is the effect of prolonged exposure at $37\text{ }^{\circ}\text{C}$ on liposome-PNIPA hydrogel nanoparticles. Corresponding size data from DLS are shown in Figure 6. Each data point corresponds to the average D_h and standard variation from a 2.5 min measurement run. After 7.5 min exposure at $37\text{ }^{\circ}\text{C}$, the average D_h increased significantly, which is indicative of nanoparticle aggregation. Similar behavior has also

been previously reported³⁴ for bulk-prepared liposome-PNIPA particles. The increasing hydrophobicity of the PNIPA gel cores is believed to drive such aggregation.

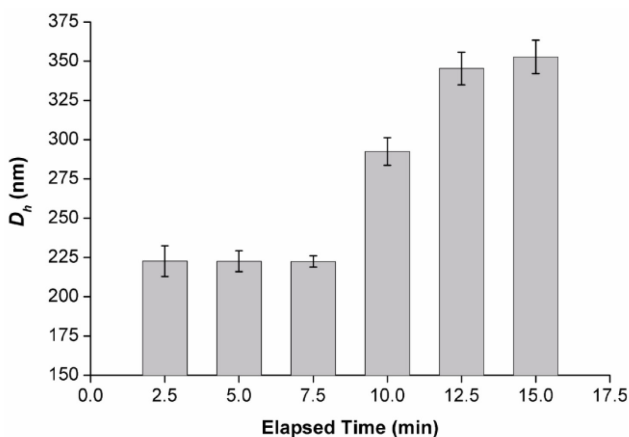


Figure 7. Time-lapse DLS data showing the effect of prolonged exposure to 37 °C on the hydrodynamic diameter D_h of liposome-PNIPA nanoparticles (VFRR of 10:1).

Stability of Liposome-PNIPA Nanoparticles.

Liposome-PNIPA nanoparticles were monitored for stability after formation. Fluorescence micrographs of particles two weeks after formation (Figure 8a) confirm that the particles are discrete and unaggregated. TEM measurements in Figure 8b show hybrid nanoparticles made at a VFRR 15:1 after two months. The nanoparticles generally show the same solid, spherical structure as the initially polymerized sample shown in Figure 5b, further confirming their stability and robustness. DLS measurements made on samples after 4 months also verified that the sizes remained consistent, which is likely due to the lipid bilayer coating preventing aggregation of the PNIPA nanogel cores. It should be noted that the DCP component of the lipid formulation has a negative charge, which confers electrostatic stability to the resulting liposomes as well as to the liposome-PNIPA nanoparticles.

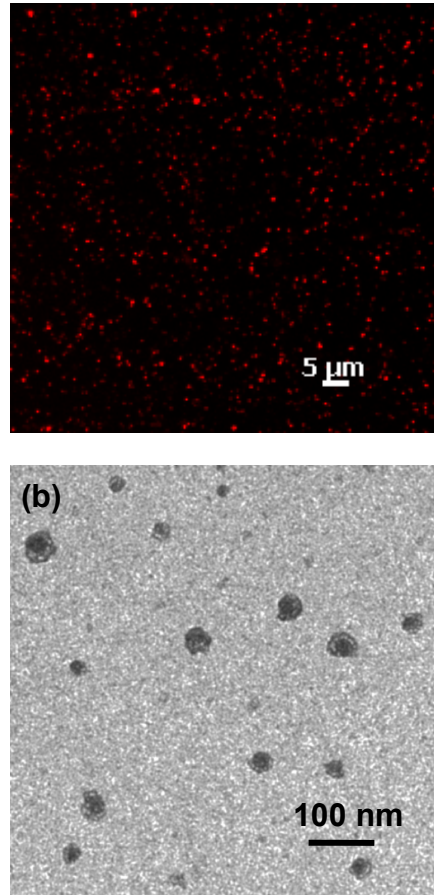


Figure 8. Stability of the liposome-PNIPA hybrid nanoparticles: (a) Epifluorescence micrograph taken two weeks after sample formation shows that the nanoparticles remain unaggregated. (b) TEM of the VFRR 15:1 sample two months after formation shows that the particles still retain similar structure and size, comparable to the original sample in Figure 5b.

Bulk preparations of lipid-hydrogel nanoparticles typically involve the use of a single formulation of lipid and hydrogel precursor to produce a single vesicle population with a particular size distribution determined by the application of several size-altering post-processing steps, which can decrease yield, increase preparation time, and introduce biological compatibility issues. Using our microfluidic method, we synthesized relatively monodisperse populations of liposome-PNIPA hybrid nanoparticles from a single

formulation without size-altering post-processing. Through precise variation of microfluidic mixing conditions, our method should be able to produce nanoparticle populations with any intended average size within some finite range from an initial formulation, limited primarily by the chemical compatibility of the precursor solutions at the fluidic interface. If necessary, following nanoparticle synthesis the IPA used in our method can be removed by dialysis to prevent potentially toxic effects. Our approach could be useful in therapeutic agent delivery and cellular uptake applications, which often require different carrier materials and sizes to target different types of cells.

With the many polymers and lipids commercially available and the interest in tailoring different types of nanoparticles for various applications⁴³, the development of a more standardized and controlled formation method such as the presented model system would be advantageous. We expect that this system could be adapted and optimized for the microfluidic-directed synthesis of hybrid nanoparticles derived from other soft matter precursors of present interest³⁴.

Conclusion

We have demonstrated a microfluidic method to direct the assembly of liposome-PNIPA hybrid nanoparticles. By varying microfluidic mixing conditions, we were able to control the size of the liposome molds that encapsulated the gel precursor, which thereby determined the sizes of the resultant hybrid nanoparticles. Using light scattering and TEM, we verified that our method produced narrowly dispersed populations of lipid-hydrogel hybrid nanoparticles over a size range pertinent to targeted delivery and controlled release applications. Our method can be further improved through on-chip integration of the off-chip formation steps; however the main objective of our work is to demonstrate the utility of a microfluidic-directed approach towards hybrid nanoparticles. We believe that this microfluidic approach may be customized for the synthesis of a wide variety of soft nanoparticles that are currently prepared via bulk methods.

Acknowledgements

This research was performed while SMS held a National Research Council Research Associateship Award at the National Institute of Standards and Technology (NIST). Device fabrication was performed in part at the Cornell Nanoscale Science and Technology Facility (CNF), a member of the National Nanotechnology Infrastructure Network supported by the NSF, and in part at the NIST Center for Nanoscale Science and Technology (CNST). The authors would like to thank the CNF and CNST staff for assistance with device fabrication, Wyatt Vreeland from the NIST Biochemical Science Division for use of the AF4-MALLS instrumentation, and Jon Geist and Darwin Reyes from the NIST Semiconductor Electronics Division for helpful discussions.

References

- [1] Torchilin, V. P. "Multifunctional nanocarriers." *Advanced Drug Delivery Reviews* 2006, 58, 1532-1555.
- [2] Jin, T.; Pennefather, P.; Lee, P. I. "Lipobeads: A hydrogel anchored lipid vesicle system." *FEBS Letters* 1996, 397, 70-74.
- [3] Agrawal, A.; Deo, R.; Wang, G. D.; Wang, M. D.; Nie, S. M. "Nanometer-scale mapping and single-molecule detection with color-coded nanoparticle probes." *Proceedings of the National Academy of Sciences of the United States of America* 2008, 105, 3298-3303.
- [4] Hu, Z. B.; Lu, X. H.; Gao, J.; Wang, C. J. "Polymer gel nanoparticle networks." *Advanced Materials* 2000, 12, 1173-1176.
- [5] Kim, J. S.; Rieter, W. J.; Taylor, K. M. L.; An, H.; Lin, W. L.; Lin, W. B. "Self-assembled hybrid nanoparticles for cancer-specific multimodal imaging." *Journal of the American Chemical Society* 2007, 129, 8962-8963.
- [6] Schillemans, J. P.; Flesch, F. M.; Hennink, W. E.; van Nostrum, C. F. "Synthesis of bilayer-coated nanogels by selective cross-linking of monomers inside liposomes." *Macromolecules* 2006, 39, 5885-5890.
- [7] Raemdonck, K.; Demeester, J.; De Smedt, S. "Advanced nanogel engineering for drug delivery." *Soft Matter* 2009, 5, 707-715.
- [8] Fenart, L.; Casanova, A.; Dehouck, B.; Duhem, C.; Slupek, S.; Cecchelli, R.; Betbeder, D. "Evaluation of effect of charge and lipid coating on ability of 60-nm nanoparticles to cross an in vitro model of the blood-brain barrier." *Journal of Pharmacology and Experimental Therapeutics* 1999, 291, 1017-1022.
- [9] Sanvicens, N.; Marco, M. P. "Multifunctional nanoparticles - properties and prospects for their use in human medicine." *Trends in Biotechnology* 2008, 26, 425-433.
- [10] Thevenot, J.; Troutier, A. L.; David, L.; Delair, T.; Ladaviere, C. "Steric stabilization of lipid/polymer particle assemblies by poly(ethylene glycol)-lipids." *Biomacromolecules* 2007, 8, 3651-3660.
- [11] Rondeau, E.; Cooper-White, J. J. "Biopolymer microparticle and nanoparticle formation within a microfluidic device." *Langmuir* 2008, 24, 6937-6945.

- [12] Lewinski, N.; Colvin, V.; Drezek, R. "Cytotoxicity of nanoparticles." *Small* 2008, 4, 26-49.
- [13] Ferdous, A. J.; Stembridge, N. Y.; Singh, M. "Role of monensin PLGA polymer nanoparticles and liposomes as potentiator of ricin A immunotoxins in vitro." *Journal of Controlled Release* 1998, 50, 71-78.
- [14] An, S. Y.; Bui, M. P. N.; Nam, Y. J.; Han, K. N.; Li, C. A.; Choo, J.; Lee, E. K.; Katoh, S.; Kumada, Y.; Seong, G. H. "Preparation of monodisperse and size-controlled poly(ethylene glycol) hydrogel nanoparticles using liposome templates." *Journal of Colloid and Interface Science* 2009, 331, 98-103.
- [15] Kabanov, A. V.; Vinogradov, S. V. "Nanogels as pharmaceutical carriers: finite networks of infinite capabilities." *Angewandte Chemie-International Edition* 2009, 48, 5418-5429.
- [16] Xu, Q. B.; Hashimoto, M.; Dang, T. T.; Hoare, T.; Kohane, D. S.; Whitesides, G. M.; Langer, R.; Anderson, D. G. "Preparation of monodisperse biodegradable polymer microparticles using a microfluidic flow-focusing device for controlled drug delivery." *Small* 2009, 5, 1575-1581.
- [17] Jiang, W.; Kim, B. Y. S.; Rutka, J. T.; Chan, W. C. W. "Nanoparticle-mediated cellular response is size-dependent." *Nature Nanotechnology* 2008, 3, 145-150.
- [18] Farokhzad, O. C.; Langer, R. "Impact of nanotechnology on drug delivery." *Acs Nano* 2009, 3, 16-20.
- [19] Knight, J. B.; Vishwanath, A.; Brody, J. P.; Austin, R. H. "Hydrodynamic focusing on a silicon chip: mixing nanoliters in microseconds." *Physical Review Letters* 1998, 80, 3863-3866.
- [20] Jahn, A.; Vreeland, W. N.; Gaitan, M.; Locascio, L. E. "Controlled vesicle self-assembly in microfluidic channels with hydrodynamic focusing." *Journal of the American Chemical Society* 2004, 126, 2674-2675.
- [21] Karnik, R.; Gu, F.; Basto, P.; Cannizzaro, C.; Dean, L.; Kyei-Manu, W.; Langer, R.; Farokhzad, O. C. "Microfluidic platform for controlled synthesis of polymeric nanoparticles." *Nano Letters* 2008, 8, 2906-2912.
- [22] Wong, H. L.; Rauth, A. M.; Bendayan, R.; Manias, J. L.; Ramaswamy, M.; Liu, Z. S.; Erhan, S. Z.; Wu, X. Y. "A new polymer-lipid hybrid nanoparticle system increases cytotoxicity of doxorubicin against multidrug-resistant human breast cancer cells." *Pharmaceutical Research* 2006, 23, 1574-1585.

- [23] Zhang, L.; Chan, J. M.; Gu, F. X.; Rhee, J.-W.; Wang, A. Z.; Radovic-Moreno, A. F.; Alexis, F.; Langer, R.; Farokhzad, O. C. "Self-assembled lipid-polymer hybrid nanoparticles: a robust drug delivery platform." *ACS Nano* 2008, 2, 1696-1702.
- [24] Wong, H. L.; Bendayan, R.; Rauth, A. M.; Wu, X. Y. "Development of solid lipid nanoparticles containing ionically complexed chemotherapeutic drugs and chemosensitizers." *Journal of Pharmaceutical Sciences* 2004, 93, 1993-2008.
- [25] Kohane, D. S. "Microparticles and nanoparticles for drug delivery." *Biotechnology and Bioengineering* 2007, 96, 203-209.
- [26] Liu, J. W.; Stace-Naughton, A.; Jiang, X. M.; Brinker, C. J. "Porous nanoparticle supported lipid bilayers (protocells) as delivery vehicles." *Journal of the American Chemical Society* 2009, 131, 1354-+.
- [27] Hong, J. S.; Vreeland, W. N.; DePaoli Lacerda, S. H.; Locascio, L. E.; Gaitan, M.; Raghavan, S. R. "Liposome-templated supramolecular assembly of responsive alginate nanogels." *Langmuir* 2008, 24, 4092-4096.
- [28] Kazakov, S.; Kaholek, M.; Teraoka, I.; Levon, K. "UV-induced gelation on nanometer scale using liposome reactor." *Macromolecules* 2002, 35, 1911-1920.
- [29] Monshipouri, M.; Rudolph, A. S. "Liposome-encapsulated alginate - controlled hydrogel particle formation and release." *Journal of Microencapsulation* 1995, 12, 117-127.
- [30] Van Thienen, T. G.; Lucas, B.; Flesch, F. M.; van Nostrum, C. F.; Demeester, J.; De Smedt, S. C. "On the synthesis and characterization of biodegradable dextran nanogels with tunable degradation properties." *Macromolecules* 2005, 38, 8503-8511.
- [31] Kazakov, S.; Kaholek, M.; Kudasheva, D.; Teraoka, I.; Cowman, M. K.; Levon, K. "Poly(N-isopropylacrylamide-co-1-vinylimidazole) hydrogel nanoparticles prepared and hydrophobically modified in liposome reactors: atomic force microscopy and dynamic light scattering study." *Langmuir* 2003, 19, 8086-8093.
- [32] Patton, J. N.; Palmer, A. F. "Photopolymerization of bovine hemoglobin entrapped nanoscale hydrogel particles within liposomal reactors for use as an artificial blood substitute." *Biomacromolecules* 2005, 6, 414-424.
- [33] Vihola, H.; Laukkanen, A.; Valtola, L.; Tenhu, H.; Hirvonen, J. "Cytotoxicity of thermosensitive polymers poly(N-isopropylacrylamide),

- poly(N-vinylcaprolactam) and amphiphilically modified poly(N-vinylcaprolactam).” *Biomaterials* 2005, 26, 3055-3064.
- [34] Kazakov, S.; Levon, K. “Liposome-nanogel structures for future pharmaceutical applications.” *Current Pharmaceutical Design* 2006, 12, 4713-4728.
- [35] Jahn, A.; Stavis, S. M.; Hong, J. S.; Vreeland, W. N.; DeVoe, D. L.; Gaitan, M. “Microfluidic mixing and the formation mechanism of nanoscale lipid vesicles.” *Manuscript submitted for publication*. 2009.
- [36] Hamidi, M.; Azadi, A.; Rafiei, P. “Hydrogel nanoparticles in drug delivery.” *Advanced Drug Delivery Reviews* 2008, 60, 1638-1649.
- [37] Certain commercial materials and equipment and identified in order to specify adequately experimental procedures. In no case does such identification imply recommendation or endorsement by the National Institute of Standards and Technology, nor does it imply that the items identified are necessarily the best available for the purpose.
- [38] Korgel, B. A.; van Zanten, J. H.; Monbouquette, H. G. “Vesicle size distributions measured by flow field-flow fractionation coupled with multiangle light scattering.” *Biophysical Journal* 1998, 74, 3264-3272.
- [39] Wyatt, P. J. “Submicrometer particle sizing by multiangle light scattering following fractionation.” *Journal of Colloid and Interface Science* 1998, 197, 9-20.
- [40] Jahn, A.; Vreeland, W. N.; DeVoe, D. L.; Locascio, L. E.; Gaitan, M. “Microfluidic directed formation of liposomes of controlled size.” *Langmuir* 2007, 23, 6289-6293.
- [41] Liu, Q. F.; Zhang, P.; Qing, A. X.; Lan, Y. X.; Lu, M. G. “Poly(N-isopropylacrylamide) hydrogels with improved shrinking kinetics by RAFT polymerization.” *Polymer* 2006, 47, 2330-2336.
- [42] Kratz, K.; Hellweg, T.; Eimer, W. “Structural changes in PNIPAM microgel particles as seen by SANS, DLS, and EM techniques.” *Polymer* 2001, 42, 6631-6639.
- [43] Moghimi, S. M.; Hunter, A. C.; Murray, J. C. “Long-circulating and target-specific nanoparticles: theory to practice.” *Pharmacological Reviews* 2001, 53, 283-318.